Research on Low Resolution Digital Image Reconstruction Method Based on Rational Function Model

Xinling Feng, Cuiqing Zhu, Zixia Ge

***Abstract*—In order to improve the visualization effect of low resolution digital images, this study proposes a low resolution digital image reconstruction method based on Rational Function Model. Firstly, bilateral filtering is employed to preprocess low resolution digital images for denoising with preservation of considerable edge details of the images. Secondly, to make the digital images unlimited to the coordinate system in the reconstruction process, a Rational Function Model with general attributes is constructed. Data obtained from the model is taken as the input information, and the generative adversarial network is used to extract image features, which lays the data foundation for subsequent image reconstruction. Thirdly, SIFT algorithm and Difference of Gaussians function are used for accurate feature extraction to compensate for the extraction deviation caused by the defects of the training set itself in the generative adversarial network. Finally, the processes of feature point direction matching, wavelet transform, bilateral regularization processing, pixel correction, edge adaptive processing, etc. are carried out for ortho correction of the image function model. On this basis, image reconstruction is eventually established. The experiment shows the edges of the reconstructed digital image are non-aliased and relatively smooth, and the texture direction and shape in the original image are well maintained, so that the details of the target parts are greatly preserved, with high accuracy of feature point matching. Furthermore, the peak signal-to-noise ratio of the reconstructed digital image ranges from 90.3dB to 92.7dB, and the structural similarity index varies from 0.93 to 0.96, further demonstrating the effectiveness of this method.**

***Index Terms*—Low resolution digital images, Bilateral filtering, Rational function model, Generative adversarial network, Image feature extraction, Image reconstruction**

I. Introduction

Digital image refers to an image that is discretely described by digital coding. It is a matrix composed of pixels, and each pixel has a digital value to represent its attributes. Compared with traditional analog images, digital images can not only be easily copied and shared, greatly facilitating the dissemination and use of images, but also be analyzed and recognized through mathematical models and algorithms, achieving automatic image processing and intelligent applications.

In some application scenarios, however, influenced by lighting conditions, device quality, and environmental noise, collected images may be poor in quality, resulting in low resolution digital images. With the continuous development of digital image technology, more and more application scenarios require reconstruction and enhancement of low resolution images [1, 2]. Low resolution digital image reconstruction method has now become an important research direction in digital image processing, which seeks to reconstruct low resolution images into high-resolution ones with prior knowledge and statistical models to improve image quality and resolution [3].

The research on low resolution digital image reconstruction is of great significance. For some application scenarios that require high-resolution image support, such as medical image diagnosis, satellite remote sensing image analysis, security monitoring, etc., low resolution image reconstruction technology can help us obtain more detailed information from blurred images, and improve image clarity and accuracy [4]. In addition, this technology can also reduce costs and improve efficiency to a certain extent. As in certain scenarios, acquisition and storage of high-resolution images consumes a large amount of resources and time.

Therefore, an illumination enhancement function with color restoration and edge preservation is introduced in reference [5], trying to enhance the poor effectiveness in low illumination environments and improve the saliency of image texture features. After preliminary image processing, the image is processed through Weighted Least Squares (WSL) filter to suppress the attenuation of high-frequency features in the image. On this basis, an edge preserving illuminance enhancement function is used to estimate the reflection component of the image, estimate the estimation results, and further enhance the texture features during the image reconstruction process. A multi-level low-light image super-resolution reconstruction method based on gradient orientation consistency is established in reference [6]. The robust map algorithm is used to eliminate the interference of grayscale gradient fluctuations on image quality, and segmentation is then performed in line with the lateral gradient of image quality, thus achieving effective image quality-based extraction. On this basis, the gradient values in

Manuscript received June 20, 2023; revised November 28, 2023. This work was supported by Changzhou Sci&Tech Program (CE20235043).

Xinling Feng is a lecturer at the School of Computer Engineering, Jiangsu University of Technology, Changzhou 213001, China. (corresponding author to provide phone: +86-519-86953240, fax: +86-519-86953240, e-mail: fengxl@jsut.edu.cn).

Cuiqing Zhu is a lecturer at the School of Computer Engineering, Jiangsu University of Technology, Changzhou 213001, China. (e-mail: zcq@jsut.edu.cn).

Zixia Ge is an experimentalist at the school of Electrical & Information Engineering, Jiangsu University of Technology, Changzhou 213001, China. (e-mail: gzx@jsut.edu.cn).

the adjacent orthogonal directions are used to synthesize those in the horizontal and vertical directions, which are used as auxiliary indexes to adaptively adjust themselves to minimize the fitting deviation and reconstruct the contour of the target. Then inconsistent interpolation enhancement techniques are employed to preserve the original color, and color restoration coefficients are used to solve the problem of color imbalance and distortion. Finally, the constraint method of consistent main directions of multi-scale gradients is applied to establish a multi-scale reflection component projection matrix, aiming to achieve the reconstruction of low resolution images. Reference [7] puts forward a low resolution image reconstruction method based on visual communication technology. This method first classifies and segments images in terms of sensitivity differences to ensure the image accuracy, thereby obtaining images with higher substantive effects. Then, the ultrahigh differential rate reconstruction technology based on the compression sensing principle is used to reconstruct the high-precision, high-quality and high-quality laser imaging. Meanwhile, the secondary iterative compression algorithm based on total variation regularization is applied to improve the edge quality of the reconstructed image.

However, practical applications with above methods demonstrate that the peak signal-to-noise ratio and structural similarity index of the reconstructed digital images are relatively small. To solve this problem, this study proposes a new low resolution digital image reconstruction method based on the Rational Function Model.

II. Preprocessing of Low Resolution Digital Images

Digital images are collected by collection devices such as cameras, scanners, etc. The parameters such as the number of pixels and sampling speed of these devices determine the quality of the collected images [8]. In the process of digital image transmission and storage, images may be compressed and optimized due to limitations such as network bandwidth and storage capacity. Improper use of these technologies may lead to a decrease in image resolution [9]. In addition, reconstruction process is highly sensitive to the influence of environmental noises, giving rise to a large amount of redundant points and noise information in digital images. This directly affects the subsequent feature extraction speed and feature matching accuracy, rendering it difficult to ensure the quality and effectiveness of digital image reconstruction. Therefore, before reconstruction, it is necessary to implement filtering processing on the digital image to eliminate noise interference.

Bilateral filter (BF) is a nonlinear smoothing filtering algorithm based on optimized Gaussian filtering. It performs image denoising through smoothing filtering, while preserving a large number of edge detail features of the image, making it highly suitable for denoising digital images [10]. The specific implementation process is as follows:

The filtering of general digital images is described by the following Equation:

$$J'(x,y)=\frac{\sum_{i,j\in\mu} e(i,j)\times J(x,y)}{e_a} \tag{1}$$

In Formula (1), J and J' represent the digital images before and after noise filtering respectively; μ represents a rectangular area pixel centered on (x,y); $e(i,j)$ represents the weight of the filter at position (i,j); e_a represents the unique parameter, and $e_a=\sum_{i,j\in\mu} e(i,j)$.

The pixel values of the digital image J' obtained after bilateral filtering are:

$$\hat{G}(a,b)=\frac{\sum_Z \omega G(i,j)}{\sum_Z \omega} \tag{2}$$

In Formula (2), $G(i,j)$ represents the grayscale value at the neighboring pixel points (i,j); Z represents the size set by the filter, and the size of the filtering field is $(2Z+1)\times(2Z+1)$; ω represents the weight coefficient of the filter, which is mainly determined by the combination of spatial domain weight ω_s and digital image grayscale domain T. The calculation is as follows:

$$\omega=\omega_s\times T=\frac{|i-a|^2+|j-b|^2}{2\varepsilon_{2I}}\times\frac{|G(a,b)-G(i,j)|^2}{2\varepsilon_{2T}} \tag{3}$$

In Formula (3), ε_I and ε_T represent spatial proximity factor and gray level similarity factor respectively, which are mainly used to limit the relative spatial position and gray level change range of pixels; $G(a,b)$ represents the grayscale value of the central pixel point (a,b). The size of ε_T determines the number of pixels contained in the Gaussian function. If ε_I is too large, ε_T will implement compensation processing, which means the brightness information of high-frequency edges and non-edge brightness are not calculated, aiming to reduce the environmental noise and improve the digital image resolution.

III. Constructing Rational function model of digital image

In order to make the digital image reconstruction process unrestricted to the coordinate system, this study constructs a Rational Function Model with general attributes. Based on the two-dimensional coordinates (x,y) of any pixel in the image, its three-dimensional coordinates are defined as (x',y',z'). Then the Rational Function Model Formula based on the independent variable polynomial quotient is defined as follows:

$$\begin{cases} x=\dfrac{(x',y',z')\times\chi a^T}{b^T} \\ y=\dfrac{(x',y',z')\times\chi c^T}{d^T} \end{cases} \tag{4}$$

In Formula (4), χ represents the independent variable polynomial vector; a, b, c and d respectively represent

the matrix parameters of Rational Function Model; T represents the matrix transpose factor.

To ensure sufficient stability of model parameters and high reconstruction quality without influence of the unit dimension, the three-dimensional coordinates (x', y', z') of the pixel points are regularized using the following Equation set to obtain:

$$\begin{cases} x'_h = \dfrac{x' - x_p}{x'_c} \\ y'_h = \dfrac{y' - y_p}{y'_c} \\ z'_h = \dfrac{z' - z_p}{z'_c} \end{cases} \tag{5}$$

In Formula (5), x_p, y_p, and z_p represent the translation parameters of the corresponding coordinate points in different directions respectively; x'_c, y'_c and z'_c represent the scale parameters of the corresponding coordinate points in different directions respectively [11].

According to the pixel deviation $\varepsilon(\varepsilon_x, \varepsilon_y)$ and spatial deviation $\delta(\delta_{x'}, \delta_{y'}, \delta_{z'})$, corresponding observation values $U(u_x, u_y)$ and $G(g_{x'}, g_{y'}, g_{z'})$ can be obtained, and then a Rational Function Model is established, with formula as follows:

$$\begin{cases} \varepsilon_x = \dfrac{(g_{x'}, g_{y'}, g_{z'}) \times \mu a^T}{b^T} - u_x(\delta_{x'}, \delta_{y'}, \delta_{z'}) \\ \varepsilon_y = \dfrac{(g_{x'}, g_{y'}, g_{z'}) \times \mu c^T}{d^T} - u_y(\delta_{x'}, \delta_{y'}, \delta_{z'}) \end{cases} \tag{6}$$

It can be seen that the constructed model is a nonlinear equation related to matrix parameters a, b, c, and d. Therefore, to facilitate the minimum variance estimation and obtain the optimal parameters, the direct method is used to linearize the Rational Function Model, attempting to reduce the computational complexity and dependence on the initial values.

IV. Preliminary Extraction of Image Features Based on Generative Adversarial Network

On the basis of the low resolution digital image function model established above, the model data is taken as the input information, and the image features are extracted using the generative adversarial network, laying data foundation for subsequent image reconstruction.

Generative adversarial network includes generative network model and discriminant network model. The former generates forged images by learning the feature distribution of real images, while the latter improves its accuracy by discriminating the difference between real and forged images.

The generative adversarial network model is generated through interactive training [12]. After inputting the Rational Function Model data of the digital image, the discriminant network and generator network are then optimized, and the output result is the feature information of the digital image [13].

The objective function of generative adversarial network is as follows:

$$F = \min_L \max_K F_{(K,L)} = E_1 \times K_+ + E_2 \times L_+ \tag{7}$$

In Formula (7), $F_{(K,L)}$ represents the generative adversarial network model function, K and L represent the discriminant network model and the generated network model respectively, E_2 represents the expected value of the actual image data after passing the discriminator, E_1 represents the expected value of the actual image data after passing the generator, K_+ represents the discriminator, and L_+ represents the generator.

In designing the generator structure, first design a 9 × 9 convolutional layer to preliminarily extract the features of the digital image, then combine with the activation function to establish the feature channel through convolution processing in the WDSR-B residual block, and then expand the feature channel through convolution processing again in the CP module. After that, the feature information of the digital image is output through the output channel of the CP module, and finally the image features are fused through skip connections.

In the field of image processing, feature fusion and feature intersection share certain similarities [14]. Yet in comparison, the feature fusion process can better utilize features of different attributes, which are then jointly modeled to improve image reconstruction performance. The digital image feature information is obtained as follows:

$$C = F \sum_{x=1}^{l} \sum_{y=1}^{h} (1 - M_{lh}) + L_a - p_N \tag{8}$$

In Formula (8), l and h represent the width and height of the resolution digital image respectively; L_a represents adversarial losses; p_N represents the random noise distribution.

V. Accurate Extraction of Digital Image Features

Although the generative adversarial network can produce realistic images, certain deviations still exist. It is because the results by this network are generated based on the probability distribution of the training data set, which may be noisy, incomplete or unbalanced. These problems may lead to certain deviations in generated images, subsequently affecting the accuracy and reliability of the extracted features. In order to solve this problem, this research uses SIFT algorithm and Difference of Gaussians (DOG) function to accurately extract the feature information of digital images based on the generative adversarial network [15].

SIFT algorithm is an image feature description algorithm based on scale space invariance, which has the advantages of rotational invariance, scale invariance and strong stability. To extract image features with this algorithm is useful to enhance the efficiency and accuracy of subsequent feature matching and image reconstruction, and reduce the computational complexity of the algorithm. It is mainly divided into the following steps:

Step 1: Construct an image pyramid. By performing multi-scale feature transformation on digital images, image sequences under different scale factors are obtained. Let $Z(x,y,\varsigma_h)$ represent the scale space of the digital image, and its convolution operation result with the two-dimensional Gaussian function $H(x,y,\varsigma_h)$ with gradual scale is:

$$H(x,y,\varsigma_h)=\frac{1}{2\pi\varsigma_h^2}\exp\left(-\frac{(x-x_0)^2+(y-y_0)^2}{2\varsigma_h^2}\right) \tag{9}$$

$$Z(x,y,\varsigma_h)=H(x,y,\varsigma_h)*J' \tag{10}$$

In the above Formula, $\varsigma_o=\varsigma_o^0 2^{o+\frac{t}{d}}$ represents the Gaussian scaling function; h and t represent the number of groups and layers of the Gaussian pyramid respectively, and $o\in[0,1,...,O-1]$, $t\in[0,1,...,d+2]$; $*$ represents the convolutional operation symbol.

Continuously downsampling the digital images in the third lowest layer of the i group of the pyramid, the first layer digital image of the $i+1$ group of the pyramid can be directly obtained. The number of layers of a pyramid is determined by the size of the original digital image and the highest-level digital image [16], which can be described by the following Equation:

$$P=\log_2\left(\min(Q,M)\right)-l \tag{11}$$

In Formula (11), (Q,M) represents the size of the digital image; l represents the logarithmic value of the size of the top-level digital image, which can be expressed as $l\in\left(0,\log_2\{\min(Q,M)\}\right)$.

Step 2: Feature point detection. Compared with the gradient, angle and other characteristics of digital images, the Gaussian Laplace function has higher stability, and the scale normalized Gaussian Laplace function is closer to the Difference of Gaussians function [17]. Therefore, DOG digital images at different scales can form a Gaussian digital image difference pyramid, which can be used to detect the extreme points of digital images. Comparison of the size of each pixel on each layer of the digital image from the second layer to the second lowest layer in the DOG space with its adjacent 26 pixels produces the local extremum points of the digital image.

Step 3: Precise positioning of feature points. Through detection of the above feature points, only a set of discrete feature points canbe obtained, while in real space, the position of the feature points needs to be further determined by interpolation and fitting operations. Therefore, the sub term interpolation operation is performed on the scale function of the DOG. The Taylor expansion for any function $g(x)$ is as follows:

$$g(x)\approx g(x_0)+\frac{\wp g^T}{\wp x}x+\frac{x^T}{2}\frac{\wp^2 g}{\wp x^2}x \tag{12}$$

From this, the Taylor expansion function of the DOG function can be obtained:

$$F(E)=F(E_0)+\frac{\wp F^T}{\wp E}+\frac{E^T}{2}\frac{\wp^2 F}{\wp E^2} \tag{13}$$

In Formula (13), E represents the position vector of the extreme point. Set $F'(E)=0$ to obtain the offset vector of the extreme point:

$$\overline{E}=-\frac{\wp^2 F^{-1}(E)}{\wp E^2}\times\frac{\wp F(E)}{\wp E} \tag{14}$$

Combine Formulas (13) and (14) to obtain $F(\overline{E})$; if $F(\overline{E})$ does not reach the set threshold size, it will be removed as an unstable feature point.

In addition, to solve the high instability of extreme points of the DOG operator at the edge of digital images, this study sets a threshold of principal curvature for the extreme points on the edge. In this way, the values obtained are kept within the threshold range, and those exceeding the threshold will be eliminated.

VI. Reconstruction of Digital Images

As mentioned in the previous parts, generative adversarial network, SIFT algorithm and DOG function are applied to accurately extract the feature information of the digital image. Regarding the 3D data of the image, feature point direction matching, wavelet transform, bilateral regularization processing, pixel correction, edge adaptive processing, etc. are then employed to complete the orthorectification of the image function model, on which, the image reconstruction is finally established.

Step 1: Match the direction of feature points.

After obtaining the position information of feature points, directional positioning analysis on the feature points is conducted to ensure the stability of the feature points during the rotation process [18]. First, take the current feature point as the rotation center, and calculate the gradient distribution value of the digital image within the specified neighborhood. The gradient modulus $m_{(x_i,y_i)}$ and direction $\vartheta_{(x_i,y_i)}$ of the feature point at (x_i,y_i) are as follows:

$$m_{(x_i,y_i)}=\sqrt{\begin{matrix}\left(Z(x_i+1,y_i)-Z(x_i-1,y_i)\right)^2\\+\left(Z(x_i,y_i+1)-Z(x_i,y_i-1)\right)^2\end{matrix}} \tag{15}$$

$$\vartheta_{(x_i,y_i)}=\tan^{-1}\frac{Z(x_i,y_i+1)-Z(x_i,y_i-1)}{Z(x_i+1,y_i)-Z(x_i-1,y_i)} \tag{16}$$

Divide the circular neighborhood of a given radius into 36 sub directions in order, with each sub direction containing the gradient information within 10°. The group with the highest cumulative gradient value is obtained through statistics, and the main direction of the feature points is determined through parabolic interpolation algorithm [19].

Step 2: Wavelet transform.

With the feature points of digital images matched, assume that the 3D scale function and wavelet function of the digital image with size (Q,M) are $\phi_{(x,y,z)}$ and $\partial_{(x,y,z)}$ respectively, and the following expression is used to complete the wavelet transform processing of the image features:

$$C' = \frac{C}{QM} \times \sum_{x=1}^{Q} \sum_{y=1}^{M} \phi_{(x,y,z)}^{T} \partial_{(x,y,z)}^{T} \tag{17}$$

Step 3: Bilateral regularization processing.

The data fidelity term described by the weighted terms of the first and second norm $\|L\|_1$ and $\|L\|_2$ is used to represent the constraint term of the reconstructed image using the bilateral regularization term. If the downsampling factors of the sampled images are the same, the norm weighted bilateral regularization form can be expressed as follows:

$$J_{(x,y)} = \arg\min_{(x,y)} \left\{ \varpi \sum_{x=1}^{Q} \sum_{y=1}^{M} \|L\|_1 + (1-\varpi) \sum_{x=1}^{Q} \sum_{y=1}^{M} \|L\|_2 \right\} \tag{18}$$

In Formula (18), $J_{(x,y)}$ represents the image after bilateral regularization, and ϖ represents the weighting factor.

Step 4: Image pixel correction.

In order to improve the clarity of the reconstructed digital images, the Canny operator is firstly used to detect the image edge, and then each pixel is corrected according to the blurry degree with the weighting term of the point spread function window. Given that the eight neighborhood directional gradient of the pixel (x, y) is G_{xy}, and the Point spread function window is normally distributed, the pixel correction process of the digital image is as follows:

$$(x', y') = \frac{\rho \exp\left(-\frac{x^2 + y^2}{2} \right)}{\exp\left(-\frac{\lambda |G_{xy}|}{\sum |G_{xy}|} \right)} \tag{19}$$

In Formula (19), the denominator represents the weighting function; Molecule represents Point spread function; λ, ρ represents the constant coefficients of two functions, respectively.

Step 5: Edge adaptive processing.

To alleviate the jagged mutation in the edge area of the reconstructed image, interpolation is used to assign pixel grayscale values according to the geometric duality of the initial image. On this basis, the pixel grayscale values of odd rows and columns of the image can be reconstruct as follows:

$$(x'', y'') = \sum_{x,y=1}^{Q,M} \alpha\left(2(x' + \lambda), 2(y' + \rho)\right) \tag{20}$$

In Formula (20), α represents the interpolation coefficient. By integrating the pixel grayscale of odd and even rows and columns, the occurrence of jagged mutations in the edge area of the image is avoided.

Step 6: Ortho correction.

Using the digital image Rational Function Model established in Section 3, the pixel coordinates are obtained through iteration to complete the ortho rectification of the image. In this process, the elevation parameters of any point are acquired by fitting the data. If the amplitude exceeds the allowable value range, the following Equation set is established and the corrected amplitude that meets the accuracy requirements is obtained through iterative calculation:

$$\begin{cases} x_1 = x'' + \Delta u_x \\ y_1 = y'' + \Delta u_y \end{cases} \tag{21}$$

In Formula (21), (x_1, y_1) represents the corrected coordinate value, while Δu_y and Δu_x represent the corrected amplitude of the observed coordinates in different directions.

Step 7: Outputting the reconstruction results.

Obtain the wavelet transform value C', which combines orthorectified values and digital image features, and then output the reconstructed digital image as follows:

$$R = \sum_{x_1 = y_1 = 1}^{Q,M} \frac{C' \times s}{J_{(x,y)}} \tag{22}$$

In Formula (22), s represents the number of pixels in a digital image.

VII. Experiment and Result Analysis

The following experiment is designed to verify the effect of low resolution digital image reconstruction method based on Rational Function Model in practical application.

A. Experimental design

Analyzing the quality of reconstructed images is conducted from two perspectives in this study: visual effect analysis and indicator evaluation. The former analyzes the reconstruction effect by visually observing the edges, textures, details, and other areas of the reconstructed image; the latter analyzes the reconstruction effect based on three indicators: peak signal-to-noise ratio, structural similarity index, and feature point matching effect. In the process of indicator evaluation, in order to avoid too single experimental results, the method of reference [5] and method of reference [6] are compared with the method of this paper for performance verification.

B. Visual effect analysis

The visual evaluation strategy, as a highly sensory evaluation mode, helps to make the algorithm highly close to the human visual perception system, bringing better visual experience to users. Figure 1 shows two original low resolution digital images (Figure 1(a) is the building image, Figure 1(b) is the physical image of the table and chair), Figure 2 is the processed image of Figure 1, and Figure 3 is the reconstructed digital image.

Fig. 1. Original digital images

(a) (b)

Fig. 2. Digital images during processing

(a) (b)

Fig. 3. Reconstructed digital images

By comparing the edge and texture regions of the three images, it can be seen that the reconstructed digital images are smooth without jagged edges. Besides, they maintain the texture directions and shapes in the original images well without deformation or distortion, so that the details of the target parts are highly preserved. The results in Figure 3 show that the method of this paper builds a Rational Function Model for building digital images on the basis of preprocessing low resolution digital images. By regularizing the Rational Function Model, the model parameters are sufficiently stable, thus effectively eliminating artifacts such as aliasing, pixel blocks, blurring, which greatly improves the reconstruction quality and visual effect of digital images.

C. Indicator evaluation analysis

Following the above visual analysis of the reconstruction effect by the proposed method in this paper, the reconstruction effects by this method, method of reference [5], and method of reference [6] are further analyzed from three aspects: feature point matching effect, peak signal-to-noise ratio, and structural similarity index.

1) Analysis of feature point matching effect

With a binocular camera to collect digital images, the experiment employs method of this paper, method of reference [5], and method of reference [6] to perform feature point matching tests. If the feature points match correctly, they are displayed as blue segments; otherwise they are displayed as red segments. The matching results of digital image feature points obtained in this way are shown in Figure 4.

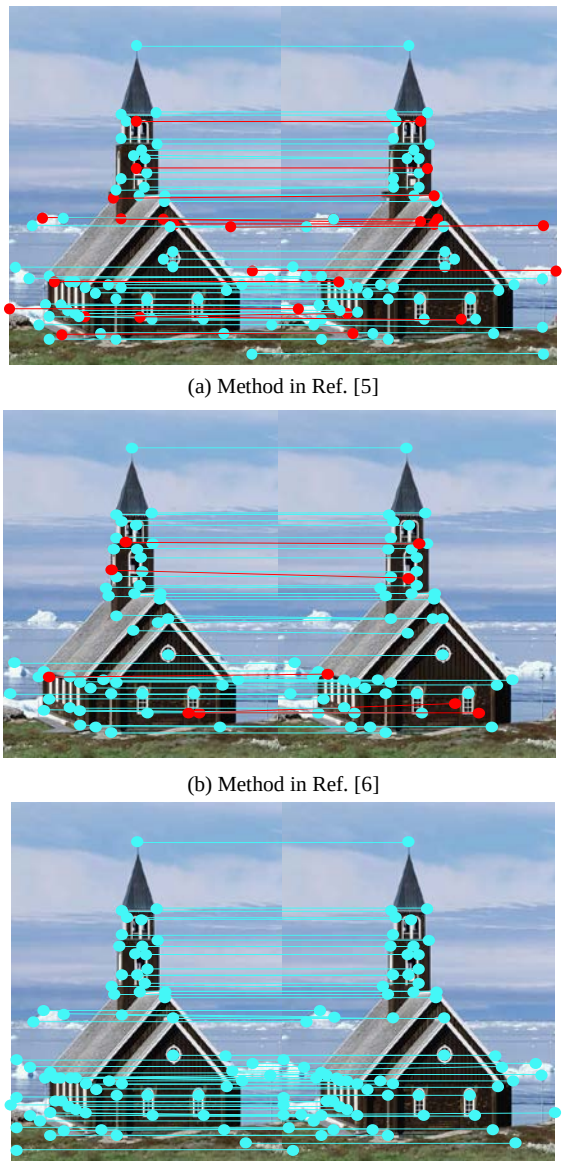

(a) Method in Ref. [5]

(b) Method in Ref. [6]

(c) Our method

Fig. 4. Matching results of feature point pairs using different methods

Figure 4 (a) reveals that the method of reference [5] has a wide detection range of feature points, but there are many mismatched points and dense clusters, which influences the reconstruction effect of subsequent images. The feature point matching accuracy of method of reference [6] is higher than that of method of reference [5], but the detection range is small, making it difficult to achieve comprehensive recognition and matching of digital image features; Compared with the other two traditional methods, the method of this paper can expand the range of feature detection, and present good detection results for all regions of digital images. It also has a higher accuracy in feature point matching and effectively avoids the overlap of feature points.

2) Peak signal-to-noise ratio

The peak signal-to-noise ratio (PSNR) of the reconstructed image is usually used to measure the similarity between the original image and the reconstructed image. It can be calculated by the following formula:

$$PSNR = \lg \frac{QM \times f_{\max}}{\sum_{x=1}^{Q}\sum_{y=1}^{M}[M-R]^2} \tag{23}$$

In Formula (23), M represents the initial laser image, R represents the reconstructed image, and $f_{\max}$ represents the maximum grayscale value of the laser image.

The peak signal-to-noise of reconstructed digital images using different methods is shown in Table I.

TABLE I
COMPARISON OF PEAK SIGNAL TO NOISE RATIO OF DIFFERENT METHODS (dB)

Experimental groups	Method in Ref. [5]	Method in Ref. [6]	Method in this paper
1	79.4	80.4	91.6
2	80.5	78.7	91.7
3	77.2	82.5	92.2
4	78.3	84.6	90.3
5	81.9	82.7	91.8
6	77.5	81.6	92.7

Results in Table I reveal that in multiple experiments, the PSNR of the reconstructed digital images in reference [5] ranges from 77.2dB-81.9dB; that of method in reference [6] changes from 78.7dB to 84.6dB; and that of our method varies from 90.3dB to 92.7dB. Comparison of the numerical values shows that the PSNR by the proposed method is largely higher, indicating that our method can greatly improve the similarity between the reconstructed images and the original ones.

3) Structural similarity index

The structural similarity index (SSIM) of the reconstructed image can be used to measure the similarity between the original image and the reconstructed image, which can be calculated by the following formula:

$$SSIM = \frac{\left(2I_x I_y + C_1\right)\left(2\sigma_x\sigma_y + C_2\right)}{\left(I_x^2 I_y^2 + C_1\right)\left(\sigma_x^2 + \sigma_y^2 + C_2\right)} \tag{24}$$

In Formula (24), $\left(I_x, I_y\right)$ and $\left(\sigma_x, \sigma_y\right)$ represent the brightness and contrast of pixels (x, y) respectively, while C_1 and C_2 represent constant terms ensuring that the denominator is not zero.

The structural similarity index of reconstructed digital images using different methods is shown in Table II.

TABLE Ⅱ
COMPARISON OF STRUCTURAL SIMILARITY INDICES BETWEEN DIFFERENT METHODS

Experimental groups	Method in Ref. [5]	Method in Ref. [6]	Method in this paper
1	0.77	0.75	0.95
2	0.82	0.80	0.95
3	0.80	0.83	0.94
4	0.77	0.74	0.96
5	0.78	0.80	0.93
6	0.79	0.79	0.96

Results shown in Table II tell that in multiple experiments, the SSIM of the reconstructed digital images in reference [5] ranges from 0.77 to 0.80; that of method in reference [6] varies from 0.74 to 0.83; and that of our method changes from 0.93 to 0.96. By comparing the numerical values, it can be found that the SSIM of the digital image reconstructed in this paper is higher, indicating that the reconstruction effect of our method is better.

VIII. CONCLUSION

The purpose of this study is to improve the visualization effect of low resolution digital images. On the basis of preprocessing low resolution digital images by using bilateral filtering, a Rational Function Model with universal attributes is constructed, so that digital images are not limited to coordinate system in the reconstruction process. Then, the model data is used as input information, and image features are extracted by using the generative adversarial network, SIFT algorithm and Difference of Gaussians function to lay the data foundation for subsequent image reconstruction. Finally, image reconstruction is achieved through processes such as feature point direction matching, wavelet transform, bilateral regularization processing, pixel correction, and edge adaptive processing.

Experimental results reveal that this method effectively maintains the texture direction and shape in the original images, with high accuracy in feature point matching, allowing for high preservation of the details of the target parts. With application of this method, the PSNR of the reconstructed digital images ranges from 90.3dB to 92.7dB, and the SSIM varies from 0.93 to 0.96. The numerical results demonstrate the effectiveness of this method.

REFERENCES

[1] H. C. Qu, B. W. Tang, and G. S. Yuan, "Improved super-resolution image reconstruction algorithm," Laser & Optoelectronics Progress, vol. 58, no. 2, pp. 191-200, 2021.

[2] M. J. Gao, C. Y. Peng, Q. Y. Chang, Q. C. Yan, P. Chen, Y. C. Shang, and L. Z. Wang, "Pixel correlation interpolation micro-scanning image reconstruction technology for the thermal microscope imaging system," Optical Technique, vol. 47, no. 2, pp. 231-237, 2021.

[3] X. H. Chen, J. S. Wang, Y. L. Ruan, S. Z. Gao, "An Improved Iris Recognition Method Based on Discrete Cosine Transform and Gabor Wavelet Transform Algorithm," Engineering Letters, vol. 27, no. 4, pp. 676-685, 2019.

[4] J. Wu, Z. C. Li, J. W. Zheng, J. Xu, and Z. J. Yu, "Three-point light pen space coordinate measurement based on light field epipolar plane image ranging,' Acta Optica Sinica, vol. 40, no. 5, pp. 111-118, 2020.

[5] L. Guo, L. L. Chen, D. Q. Cheng, M. Jiang, Q. Q. Kou, and J. S. Qian, "Super resolution of low illumination image based on color restoration and edge preserving," Application Research of Computers, vol. 39, no. 4, pp. 1253-1258+1264, 2022.

[6] X. J. Zhao, and R. W. Li, "Super-resolution reconstruction model of multilevel low illumination image under constraint of gradient direction consistency," Modern Electronics Technique, vol. 45, no. 23, pp. 55-59, 2022.

[7] G. Y. Wen, "Low resolution laser image reconstruction based on visual communication technology," Laser Journal, vol. 42, no. 10, pp. 87-92, 2021.

[8] J. Jin, L. L. Dong, X. Ding, Y. H. Jiang, and W. H. Xu, "Image multiresolution reconstruction algorithm based on weighted wavelet transform," Journal of Optoelectronics Laser, vol. 30, no. 11, pp. 1215-1223, 2019.

[9] S. X. Yu, L. M. Hu, X. D. Zhang, and X. W. Fu, "Color image multi-scale guided depth image super-resolution reconstruction," Opto-Electronic Engineering, vol. 47, no. 4, pp. 42-51, 2020.

[10] H. Z. Jing, J. L. Shi, M. Z. Qiu, Y. Qi, and W. X. Zhu, “Super-resolution reconstruction method for space target images based on dense residual block-based GAN,” Optics and Precision Engineering, vol. 30, no. 17, pp. 2155-2165, 2022.
[11] Y. Q. Li, and J. J. Wang, "Edge feature extraction method of Brillouin scattering spectral image[J]," Optical Communication Technology, vol. 45, no. 3, pp. 37-41, 2021.
[12] L. H. Wang, T. Wang, Y. Zhang, X. N. Li, and L. J. Dou, “Improved iterative algorithm by self-adaptive correcting characteristic value for RFM,” Journal of Geomatics Science and Technology, vol. 38, no. 4, pp. 374-379, 2021.
[13] G. Q. Liu, J. F. Liu, and D. H. Zhu, “Image super resolution reconstruction algorithm based on generative countermeasure network,” Chinese Journal of Liquid Crystals and Displays, vol. 36, no. 12, pp. 1720-1727, 2021.
[14] L. F. He, L. L. Su, G. B. Zhou, P. Yuan, B. F. Lu, and J. J. Yu, "Image super-resolution reconstruction based on multi-scale residual aggregation feature network[J]," Laser & Optoelectronics Progress, vol. 58, no. 24, pp. 250-259, 2021.
[15] H. X. Wu, and Z. Zhang, “Three-dimensional image reconstruction method based on absolute conic image,” Computer Simulation, vol. 38, no. 8, pp. 203-206+211, 2021.
[16] H. Hu, J. L. Zhang, B. C. Li, and Z. Y. Xu, “Compressive sensing image reconstruction algorithm based on optimized sparse representation,” Semiconductor Optoelectronics, vol. 42, no. 2, pp. 269-274, 2021.
[17] M. Yu, and C. Liu, “Single exposure light field imaging based all-in-focus image reconstruction technology,” Journal of Applied Optics, vol. 42, no. 1, pp. 71-78, 2021.
[18] Y. Liu, and C. Gu, “Two Greedy Subspace Kaczmarz Algorithm for Image Reconstruction,” IAENG International Journal of Applied Mathematics, vol. 50, no. 4, pp. 853-859, 2020.
[19] Z. H. Xi, and K. P. Yuan, “Super-Resolution Image Reconstruction Based on Residual Channel Attention and Multilevel Feature Fusion,” Laser & Optoelectronics Progress, vol. 57, no. 4, pp. 262-270, 2020.